

Determination of the response of GLAST's crystals to high-energy heavy ions

B. Blank^a, G. Bogaert^b, G. Cachel^a, D. Dumora^a, E. Grove^c, B. Giebbels^b,
J. Giovinazzo^a, M. Hellström^d, S. Incerti^a, N. Johnson^c, B. Lott^a, Th.
Reposeur^a, D. Smith^a, K. Sümmerer^d

a) Centre d' Etudes Nucléaires de Bordeaux-Gradignan, France

b) Ecole Polytechnique, France

c) Naval Research Laboratory, Washington D.C., USA

d) Gesellschaft für Schwerionenforschung Darmstadt, Germany

1 Presentation of the instrument

The Gamma-Ray Large-Area Space Telescope (GLAST)[1] is the next generation high-energy gamma-ray satellite, to be launched by NASA in 2006. It will mainly be devoted to studying the cosmic accelerators of relativistic particles, electrons or hadrons, and the environment in which these particles interact with matter or radiation to produce gamma rays. The cosmic accelerators are either galactic: solar flares, pulsars, supernovae remnants, microquasars... or extragalactic: active galactic nuclei, gamma-ray bursters. GLAST's predecessor, EGRET, enabled the detection of about 270 sources. A tenfold increase in this number is expected with GLAST.

GLAST's main instrument, the large area telescope, (LAT) will cover the energy range between 20 MeV and 300 GeV. For the first time, the sky will be observed beyond 10 GeV with an instrument having a large field of view (2 sr). The improvement over EGRET will be very significant: a gain of 25 in sensitivity and better angular resolution are expected, with a factor 1000 less dead time.

The LAT comprises three sub-systems:

- a tracker made of 18 layers of crossed Silicon strips interlaced with Pb converter foils, wherein the incident gamma ray converts into a e^+e^- pair,
- a CsI calorimeter (8.5 radiation lengths in thickness) sampling the electromagnetic- shower energy,
- an anticoincidence shield for vetoing charged cosmic rays.

The calorimeter and the tracker are composed of 16 elements called towers.

2 Calorimeter characteristics

The calorimeter module of each of the 16 towers comprises 8 layers of 12 CsI crystals, 32 cm x 2.7 cm x 1.9 cm in dimensions, arranged in individual cells made of carbon fibers. Each crystal is read out at each end by two photodiodes, a large one (1.5 cm²) and a small one (0.25 cm²). Each photodiode is associated with two electronic chains with different gains. The light yield from the CsI crystals is tapered so that the shower position along the crystal can be inferred from the relative amount of light measured at each end. A position resolution better than 1 mm has been demonstrated in a beam test prototype.

3 Calibration

The energy calibration of the calorimeter represents an important step towards the mission's scientific success. The energy resolution is required to be better than 10% between 100 MeV and 10 GeV and 20% beyond 10 GeV.

In orbit, the energy calibration and the instrument response monitoring will be performed by detecting cosmic-ray heavy ions (essentially C, N, O, Ne, Mg, Si and Fe). Fig. 1 displays a typical energy spectrum of carbon ions at GLAST's flight altitude, as calculated with the code CREME [2]. This spectrum is depleted at low energy due to the geomagnetic cutoff and peaks around 4 GeV/nucleon.

Within the calorimeter, the majority of ions will induce nuclear reactions with Cs or I nuclei. Those ions that don't interact will only suffer ionisation energy loss. As the ion energies are close to the minimum-ionisation energy (about 2 GeV/nucleon), the distributions of ionisation energy deposited within the calorimeter exhibit well-defined peaks, each corresponding to a different element (Fig. 2, the atomic numbers are given for the main peaks). These peaks are broad and asymmetric, but ions having energies very different from the minimum-ionisation energy can be filtered out in the analysis by means of suitable algorithms. An illustration of the results of this filtering procedure is shown in Fig. 3 for carbon and iron ions (dashed curves).

The distributions displayed in Fig. 2 and Fig. 3 are deposited-energy (E) distributions. The photodiodes glued on the crystal ends read out the

light output (L) corresponding to E , generated by the excited scintillating molecules. Unfortunately, the function dL/dE is not linear and depends on both the ion energy and atomic number [3]: the high ionisation density created around the ion path leads to quenching interactions between the excited molecules, in which part of the energy goes into non-radiative decay channels. A precise determination of the function $L(E)$ is required in order to calibrate the LAT in space. Although several studies have been devoted to determining this function at low energy, there has been very little work beyond 100 MeV/nucleon [4, 5].

For thick detectors like GLAST's crystals, dL/dE must be integrated over energy to provide for the total light deposited L . Fig. 4 displays a possible function L (calculated under the same conditions as the curves shown in Fig. 5, see below), as a function of the deposited energy for Fe ions. The labels on the curve denote different ion's incident energies per nucleon, $E_{\text{inc}}/\text{nucleon}$. The 3 branches of the curve correspond to different energy-loss regimes:

1. for $E_{\text{inc}}/\text{nucleon} < 370$ MeV, the ions are stopped within the crystal;
2. for $370 \text{ MeV} < E_{\text{inc}}/\text{nucleon} < 2$ GeV, the ions punch through the crystal, depositing an energy varying roughly as $1/E_{\text{inc}}$;
3. for $E_{\text{inc}}/\text{nucleon} > 2$ GeV, i.e. beyond the minimum-ionisation energy, the deposited energy rises again as a function of E_{inc} .

The following section summarizes the properties of CsI regarding light emission, with emphasis on the quenching effects.

4 Quenching effects in CsI(Tl)

CsI(Tl) is an alkali halide in which the main light emission takes place in the yellow band, centered near 5500 Angstroms, referred to as the Tl band. The temporal distribution of light emission exhibits a fast rise (1 ns) followed by an exponential decay associated with two different constants: $1\mu\text{s}$ and $7\mu\text{s}$. The yield of the faster component depends on the ion atomic number while that of the slower one does not.

Most models aiming to reproduce the emission process consider that part of the charge carriers created by the ionizing particle form excitons (weakly bound e-h pairs), which migrate in the lattice and recombine at activator sites, accompanied by light emission. The main emission process is assumed to be: $e+\text{Tl}^{++} \rightarrow (\text{Tl}^+)^* \rightarrow \text{Tl}^+ + h\nu$.

At low energy, the non-linear behavior of the light conversion efficiency is well described phenomenologically by means of Birk's law [6], initially

developed for organic scintillators: $dL/dE=S/(1+K_B dE/dx)$ where S is a constant and K_B is the quenching factor. The "activator-depletion hypothesis" [7] provides a simple explanation for the quenching effect: as the e-h pair density increases, the number of unoccupied Tl sites shrinks and the remnant e-h pair density cannot contribute to scintillation for lack of available Tl sites. However, numerous studies have proved that reality is more complex and that other processes are involved. These include non-radiative excitations with a probability scaling quadratically with the pair density [8] or the destruction of e-h pairs at excited activator sites [8], or merely direct recombination.

Birk's formula, which depends only on the energy loss is valid exclusively at low energy, i.e. as long as the production of δ electrons, with energy greater than 1 keV, is negligible. At higher energy, the efficiency is observed to increase with the ion Z at a given dE/dx as illustrated in Fig. 5 and 6. Fig. 5 displays the light efficiency calculated with the function proposed by Pârlog et al.[9], whose parameters have been adjusted from data obtained in a preliminary GSI test (the dashed curves correspond to energies greater than 80 MeV/nucleon, where the function's validity remains essentially untested). Fig. 6 shows a compilation of data concerning NaI(Tl), including data [4] obtained at the Bevalac with Ne, Ar and Fe beams for energies up to 550 MeV/nucleon. The increase in light efficiency with increasing Z was explained by Murray and Meyer by considering the contribution of δ electrons in addition to that of the highly-ionised primary column. As δ electrons have a range greater than the radius of the primary column (about 400 nm), they escape the column and produce light with high efficiency in the region of low pair density. At a given dE/dx , particles with greater Z have a higher velocity and are thus more likely to produce δ electrons, resulting in a higher light efficiency.

5 Goals of the experiment

As mentioned above little is known about the behavior of the function dL/dE beyond 100 MeV/nucleon for heavy ions. The scarcity of data stems from the fact that scintillation detectors are inappropriate for measuring the total energy of relativistic ions in standard nuclear physics experiments. The ion range in the detector becoming comparable to the interaction length as the ion energy increases, the probability for a ion to induce a nuclear reaction within the detector becomes exceedingly high. The primary goal of the ex-

periment is the measurement of the function $L(E,Z)$ for the ions (C, N, O, Ne, Mg, Si, Fe) used in orbit, beyond 500 MeV/nucleon. An overlap with the low energy regime (<100 MeV/nucleon) should be performed for completeness.

A test run (S240) performed in July 2000 yielded limits on the magnitude of the quenching effects, but the number of beam types (500-700 MeV/nucleon C, 700 MeV/nucleon Ni) was insufficient for a proper mapping of the function $L(E,Z)$.

The high interaction probability mentioned above brings about problems for the on-orbit calibration (as an example, about 60% of carbon ions interact inside the calorimeter) : it is crucial to reject the nuclear-reaction events (charge- or mass-changing reactions) in order to avoid the pollution of the ionisation peaks (Fig. 3). The second goal of the experiment is to test and fine tune the rejection algorithms for the reaction events, based on the change in deposited energy within adjacent layers.

6 Description of the experiment

We desire to use a large variety of ions, ranging from carbon or lighter ions to iron, having energies varying between about 100 MeV/nucleon and 1.5 GeV/nucleon or higher by fine steps, if possible with only one accelerated beam in order to be flexible and to limit the working load on the facility's operators.

For this purpose, the experiment we propose is the following: a 1.7 GeV/nucleon Ni beam impinging on a target produces reaction fragments ranging from H to Ni, which are sorted out by a fragment separator, behind which the calorimeter prototype EM (standing for Engineering Model) is installed. The GSI FFragment Separator (FRS, Fig. 7) is perfectly suited for this task: its four dipole magnets select the traversing ions according to their magnetic rigidities (proportional to the ratio p/Q , p : linear momentum, Q : ion charge) and the associated detection system provides for a very precise identification and energy measurement of the ions on an event-by-event basis. The detection system is composed of multiwire proportional counters (MWPC) supplying the ion positions, plastic scintillation detectors enabling time-of-flight measurements, and a segmented ionisation chamber, MUSIC yielding an energy-loss measurement. The EM will be positioned behind MUSIC.

At the FRS entrance, the fragment energies depend on the target thickness, which can be varied as desired, the fragment energies per nucleon being

as high as that of the beam, i.e. 1.7 GeV/nucleon, for thin targets. With a single setting of the FRS magnets, ions of many different species will be measured at the same time. Fig. 8 displays the expected yields per projectile ion of the most-abundant isotopes at the FRS exit as a function of the atomic number. In the calculation, the FRS parameters were optimized for ^{52}Fe .

Limiting the counting rate to 150 Hz will lead to more than 10^4 counts per element (including $Z=26$) in 2 hours of data taking.

Help from the GSI acquisition group will be required in order to couple the EM and FRS data acquisition systems.

7 Beam time request

Assuming 30 minutes per setting to change the magnet fields, about 10 different energies will be explored in one day of beam time, without degrader. We would like to run with the detector axis aligned with the beam (1 day) and also tilted by $\theta=30^\circ$ and $\theta=60^\circ$ (2 shifts=16 hours each) so as to test the EM response to particles penetrating off axis, which is the most likely case in space. One compound angle, $\theta=30^\circ$ and $\phi=30^\circ$, should also be used (2 shifts).

In addition, we would like to run on C, Si and Fe only for 8 hours each using the achromatic degrader (1 day in total). These data will enable us to optimize the algorithms devised to reject the reaction events for the ion species most abundant in space. High statistics is required so that atypical events can be recorded.

Including one full day to calibrate the FRS, we request 5 days of beam time in total, with a 1.7 GeV/nucleon ^{58}Ni beam.

The experiment should be completed by the end of 2003 since other calibration runs planned at SLAC in 2004 will require many technical and human resources before launch.

The data analysis will constitute the basis of a PhD thesis at CENBG.

References

- [1] GLAST Science Brochure: <http://glast.gsfc.nasa.gov/resources/brochures>.
- [2] A. J. Tylka et al., "CREME96: A Revision of the Cosmic Ray Effects on Micro-Electronics Code", IEEE Transactions on Nuclear Science, 44, 2150-2160 (1997).

- [3] W. R. Leo, Experimental techniques for Nuclear and Particle Physics (Second edition, Springer Verlag, Berlin), p. 168.
- [4] M. H. Salamon and S. P. Ahlen, Phys. Rev. B24 (1981) 5026.
- [5] S. M. Schindler et al, Proc. 18th International Cosmic Ray Conference (Bangalore, 1983), 8, 73.
- [6] J. B. Birks, The Theory and Practice of Scintillation Counting (Pergamon, New York,1964).
- [7] R. B. Murray and A. Meyer, Phys. Rev. 122 (1961) 815.
- [8] R. C. Powell and L. A. Harrah, J. Chem. 55, (1971) 1878.
- [9] M. Pârlog et al., Nuclear Instruments and Methods in Physics Research A, in press, preprints nucl-exp/0106002, nucl-exp/0106003.

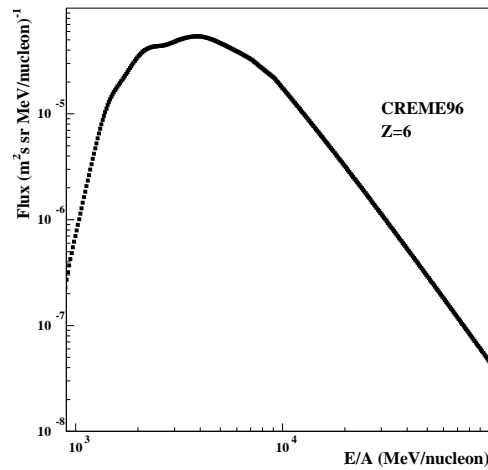


Figure 1. Energy spectrum of carbon ions at GLAST's flight altitude, as calculated with CREME.

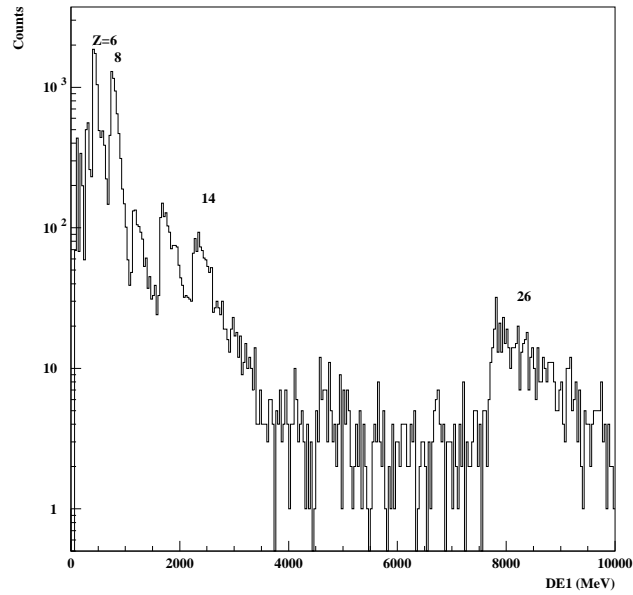


Figure 2 Expected distribution of ionisation energy deposited by the cosmic-ray ions in one CsI crystal. The main peaks are labeled according to the ion atomic numbers.

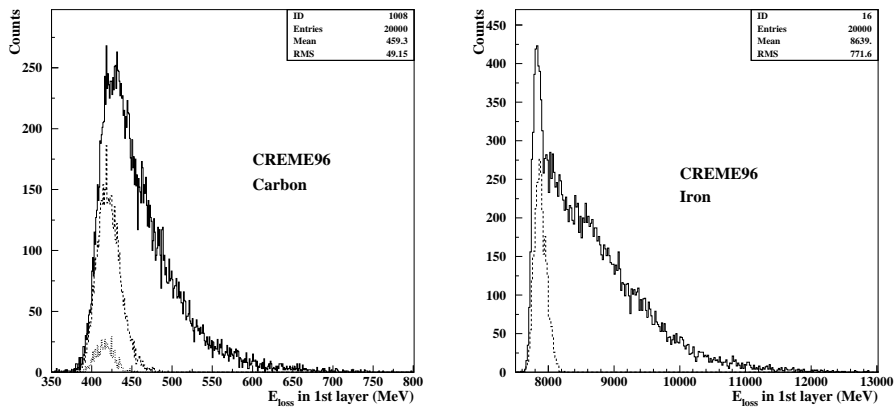


Figure 3. Distributions of ionisation-energy for carbon (left) and iron (right) ions. The dashed histograms correspond to the distributions resulting from a filtering procedure.

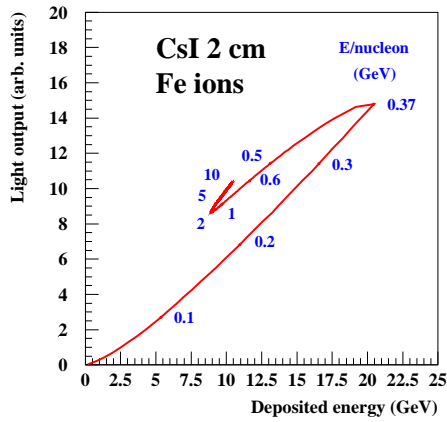


Figure 4. Possible $L(E)$ for Fe ions in a 2cm-thick CsI crystal.

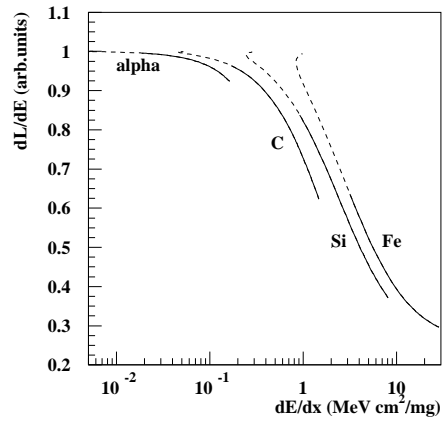


Figure 5. Calculated dL/dE as a function of dE/dx for four different ions, using the functions of ref.[9].

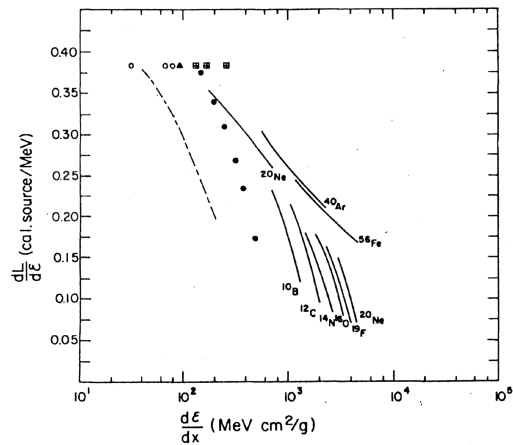


Figure 6. Compilation of experimental $dL/dE(dE/dx)$ for different ions in NaI. The open (solid) symbols and dashed curve correspond to H (He).

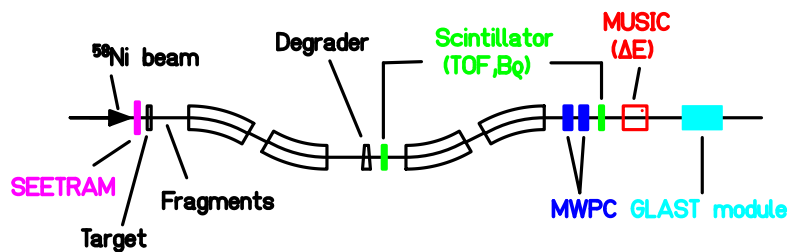


Figure 7. Sketch of the proposed experimental setup.

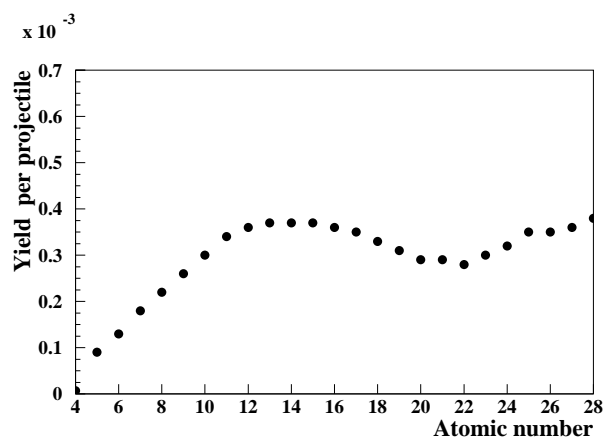


Figure 8. Calculated yield of the most abundant isotopes at the FRS exit as a function of the atomic number.